Published in final edited form as:
Bioconjug Chem. 2012 June 20; 23(6): 1322–1332. doi:10.1021/bc300175d.

A Novel Multifunctional Theranostic Liposome Drug Delivery System: Construction, Characterization, and Multimodality MR, Near-infrared Fluorescent and Nuclear Imaging

Shihong Li[†], **Beth Goins**[†], **Lujun Zhang**[‡], and **Ande Bao**[†,‡,*]

[†]Department of Radiology, University of Texas Health Science Center at San Antonio, San Antonio, Texas

[‡]Department of Otolaryngology – Head and Neck Surgery, University of Texas Health Science Center at San Antonio, San Antonio, Texas

Abstract

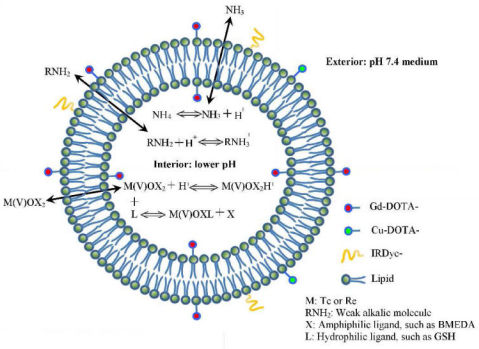

Liposomes are effective lipid nanoparticle drug delivery systems, which can also be functionalized with non-invasive multimodality imaging agents with each modality providing distinct information and having synergistic advantages in diagnosis, monitoring of disease treatment, and evaluation of liposomal drug pharmacokinetics. We designed and constructed a multifunctional theranostic liposomal drug delivery system, which integrated multimodality magnetic resonance (MR), near-infrared (NIR) fluorescent and nuclear imaging of liposomal drug delivery, and therapy monitoring and prediction. The pre-manufactured liposomes were composed of DSPC/cholesterol/Gd-DOTADSPE/DOTA-DSPE with the molar ratio of 39:35:25:1 and having ammonium sulfate/pH gradient. A lipidized NIR fluorescent tracer, IRDye-DSPE, was effectively post-inserted into the pre-manufactured liposomes. Doxorubicin could be effectively post-loaded into the multifunctional liposomes. The multifunctional doxorubicin-liposomes could also be stably radiolabeled with ^{99m}Tc or 64Cu for single photon emission computed tomography (SPECT) or positron emission tomography (PET) imaging, respectively. MR images displayed the high resolution micro-intratumoral distribution of the liposomes in squamous cell carcinoma of head and neck (SCCHN) tumor xenografts in nude rats after intratumoral injection. NIR fluorescent, SPECT and PET images also clearly showed either the high intratumoral retention or distribution of the multifunctional liposomes. This multifunctional drug carrying liposome system is promising for disease theranostics allowing non-invasive multimodality NIR fluorescent, MR,

[*]Correspondence: Department of Radiology, University of Texas Health Science Center at San Antonio, MSC 7800, 7703 Floyd Curl Drive, San Antonio, TX 78229-3900, USA. Tel: 210-567-5657; Fax: 210-567-5549; bao@uthscsa.edu.

Disclosure: No potential conflicts of interest were disclosed.

SPECT and PET imaging of their in vivo behavior and capitalizing on the inherent advantages of each modality.

Keywords

Multifunctional liposomes; Theranostics; Drug delivery; Multimodality imaging; Intratumoral retention and distribution; Nanoparticles

INTRODUCTION

Non-invasive imaging modalities, such as computed tomography (CT), magnetic resonance (MR), single photon emission computed tomography (SPECT), positron emission tomography (PET), and ultrasound (US) imaging, play key roles in clinical diagnosis, monitoring of disease status and evaluation of treatment. The optical imaging technology, especially suitable for small animals, provides a cheaper and convenient alternative to the more complicated nuclear and MR imaging modalities. Near-infrared (NIR) fluorescent probes and in vivo imaging have drawn particular interest, due to their low optical absorption and scattering by the tissue, and there is minimal tissue auto-fluorescence in the NIR window (wavelengths from 700 to 900 nm).[1] A recent clinical trial has shown that in vivo NIR fluorescent imaging could be used in lymph node mapping for surgical excision of lymph nodes in breast cancer.[2]

Each imaging modality, based on its individual mechanism of tissue contrast or function, has a specific sensitivity, spatial and temporal resolution in relationship to diseases, physiological or molecular biological procedures.[3-6] Non-invasive multimodality imaging can synergize their advantages and compensate the shortcomings of individual imaging modalities.[7-9] The use of multimodality imaging for improved disease diagnosis and therapy evaluation represents an optimal direction in radiology. In addition to the instrument innovation, new imaging tracers and probes are necessary for the development of multimodality imaging techniques. The introduction of a single platform, which integrates multiple probes to enable multimodality imaging of diseases and/or therapy response, will have advantages over a single functional probe, as each probe in the platform can afford complementary information for the other modalities. Accordingly, nanoparticle systems have shown the excellence of achieving this goal; meanwhile being used for drug delivery to advance disease treatment.[7,10-12]

The use of drug delivery systems can improve the stability, pharmacokinetics and biodistribution of a wide variety of therapeutic agents, leading to more convenient drug administration or improved treatment efficacy with decreased side effects.[7,11,12] A multifunctional drug delivery system, containing both therapeutic and imaging agents, will contribute to a more personalized cancer therapy approach by facilitating efficient delivery through image guidance and therapy response monitoring.[7] Liposomes, unilamellar lipid bilayer nanoparticles enclosing an aqueous compartment that can accommodate lipophilic or hydrophilic drug molecules, are effective drug delivery systems with an ideal construction of biocompatible, nontoxic and biodegradable materials. Liposomes can passively accumulate in tumor by extravasation through abnormal leaky tumor vasculature known as enhanced permeability and retention effect, or actively accumulate in tumor by tumor cell specific targeting or tumor angiogenic marker targeting.[13,14] Various liposome formulations have been approved by FDA for clinical cancer treatment or under trials.[15,16] Liposomes have versatile modifiability by allowing functional molecules to be encapsulated in the interior, inserted in the bilayer, or attached on the bilayer membrane surface. Thus, liposomes may be constructed to provide an ideal multi-probe platform with the capability of multimodality

theranostics. The multimodality imaging functionalization of therapeutic drug carrying liposomes is an important and necessary theranostic component for personalized monitoring of the in vivo tumor targeting and pharmacokinetics of liposomal therapeutic agents, predicting therapy outcome and gaining a better understanding of the prognosis-associated disease status by combining the advantageous information from each imaging modality.[7] For example, higher spatial resolution and better tissue contrast from MR imaging plus better quantification from nuclear imaging will provide a better understanding of the relationship of liposome formulation to associated drug effect information. Further incorporation of NIR fluorescent imaging in the liposome platform for superficial lymph node mapping will provide identification of the metastatic lymph nodes for focused lymph node treatment or guiding surgical excision.[1,2]

Herein, we have constructed a multifunctional liposomal drug delivery system comprised of DSPC/cholesterol/Gd-DOTA-DSPE/DOTA-DSPE/IRDye-DSPE with ammonium/pH gradient (Figure 1). By using the ammonium/pH gradient, this system can also be post-loaded with the most widely used gamma imaging radionuclide, technetium-99m (^{99m}Tc) ($T_{1/2}$=6.0 hr, 141 keV γ-ray),[17] the therapeutic radionuclides, rhenium-186/188 (^{186}Re/^{188}Re) [18] and weak alkalic chemotherapeutic agents, such as doxorubicin.[19] The inclusion of DOTA-DSPE in the lipid formulation enables the liposome membrane labeling of radionuclides, such as copper-64 (^{64}Cu) ($T_{1/2}$ = 12.7 hr, β^+ decay (17.4%)) [20] for PET imaging. The Gd-DOTA-DSPE component, a chelate of gadolinium (III) (Gd (III)) with lipidized macrocyclic DOTA ligand provides the liposome MR imaging capability.[21-24] The NIR fluorescent molecule, IRDye-DSPE inserted in the liposome bilayer allows NIR fluorescent imaging of tumors or tumor-associated lymph node mapping.[1,2]

Recent studies have suggested a promising regimen by direct intratumoral infusion of nanoparticle carried therapeutic agents to treat solid tumors.[25-32] To assess the multimodality imaging functions of our liposomal drug delivery system following intratumoral infusion in a squamous cell carcinoma of head and neck (SCCHN) xenograft model in nude rats, in vivo MR, NIR fluorescent, SPECT or PET images of the multifunctional liposomes with/without radiolabeling with ^{99m}Tc or ^{64}Cu, respectively, were acquired for multimodality monitoring of their in vivo behaviors including intratumoral distribution, retention and systemic distribution.

MATERIALS AND METHODS

Materials

1,2-Distearoyl-sn-glycero-3-phosphocholine (DSPC) and 1,2-distearoyl-sn-glycero-3-phosphoethanolamine (DSPE) were purchased from Avanti Polar Lipids (Alabaster, AL). Cholesterol was from Calbiochem (San Diego, CA). 1,4,7,10-Tetraazacyclododecane-1,4,7-tris(acetic acid)-10-acetic acid mono(N-hydroxysuccinimidyl ester) (DOTA-NHS ester) was from Macrocyclics (Dallas, TX). IRDye 800CW NHS ester was from LI-COR Biosciences (Lincoln, NE). Doxorubicin hydrochloride was from LC Laboratories (Woburn, MA). *N*,*N*-bis(2-mercaptoethyl)-*N'*,*N'*-diethyl-ethylenediamine (BMEDA) was from ABX GmbH (Radeberg, Germany). Sodium ^{99m}Tc-pertechnetate was from GE Healthcare (San Antonio, Texas). Carrier-free $^{153}GdCl_3$ was from PerkinElmer Life Science (Boston, MA). Carrier-free $^{64}CuCl_2$ was from University of Wisconsin– Madison (Madison, WI). GFC-04-500 gel (4% agarose crosslinked, 50-150-μm beads) was from Sooner Scientific (Garvin, OK). The HiPrep and PD-10 desalting columns were products of GE Healthcare (Piscataway, New Jersey). Ultrapure water was prepared by a Nanopure Infinity ultrapure water system (Barnstead Int., Dubuque, IA). All other chemicals were obtained from Sigma-Aldrich (St. Louis, MO).

Synthesis of DOTA-DSPE and Gd-DOTA-DSPE

A schematic diagram of the syntheses of DOTA-DSPE, Gd-DOTA-DSPE, and IRDye-DSPE is shown in Figure 2.[21,22,33] For the preparation of DOTA-DSPE, 2.0 g of DSPE was mixed with 2.3 g of DOTA-NHS ester (molar ratio, 1: 1) in a round flask, followed by the addition of 260 ml of 2% (v/v) triethylamine (TEA) in $CHCl_3$, incubation of the mixture until dissolved thoroughly and heated at 40°C for 2 hr. The obtained clear solution was concentrated by distillation under reduced pressure and dried *in vacuo*. Then, 130 ml of ultrapure water was added to dissolve the resulted product. The suspension was transferred into several 50-ml conical centrifugation tubes (Corning, Corning, NY). Each tube was exposed to 5 cycles of freezing in liquid nitrogen followed by thawing in 60°C water bath and then centrifuged at 4,500 g for 10 min. The DOTA-DSPE containing supernatant was filtered with a 0.45-μm membrane filter, and then purified with an AKTADesign FPLC system equipped with a HiPrep desalting column, a 280 nm UV detector and an automatic fraction collector (Amersham Biosciences). Ten ml of sample were loaded for each run and ultrapure water was used as mobile phase. The elution velocity was 8 ml/min. Two ml of eluate fractions were collected. Fractions 3-18 containing DOTA-DSPE, verified by UV absorption detection and thin layer chromatography with Silica gel 60 F254 plastic plate (EM Science, Gibbstown, NJ) using 64:25:4 $CHCl_3$/MeOH/water as mobile phase (DOTA-DSPE: blue spot with molybdemum spraying, Rf at 0.15, also stained by iodine exposure but negative to UV light and ninhydrin staining) were combined and lyophilized. The obtained white product was 2.80 g (93% yield).

To prepare Gd-DOTA-DSPE, DOTA-DSPE (0.384 g, 0.339 mmole) was dissolved in 38 ml of 10 mM sodium acetate buffer, pH 5.8, followed by the addition of 0.337 mmole of $Gd(OAc)_3$ in 3.1 ml water containing 3 kBq (0.081 μCi) $^{153}GdCl_3$ radioactive tracer.[20] The pH of solution was adjusted to 6.5 with 1 M NaOH. The opaque solution was heated at 50°C for 5 hr. Then, the resulted product was centrifuged at 4,500 g for 10 min. The obtained precipitate was washed sequentially 2 times with 10 ml 50 mM sodium acetate buffer, pH 5.8 followed by 10 ml water. The precipitate was then lyophilized and measured for ^{153}Gd radioactivity with an automatic Minaxiγ A5550 gamma counter (Packard, Downers Grove, Illinois). The final white product was 0.40 g, corresponding to 92% yield, which also matched the yield calculated from ^{153}Gd tracer measurement.

The DOTA-DSPE and Gd-DOTA-DSPE products were also verified by MALDI-TOF MS assay using 2,5-dihydroxybenzoic acid (DHB) matrix (Applied Biosystems Voyager DE PRO MALDITOF mass spectrometer). (DOTA-DSPE: m/z in positive mode. $[M-C_{17}H_{35}CO+H]^+$: 868.0; $[M+H]^+$: 1134.1; Gd-DOTA-DSPE: m/z in negative mode. $[868.0+Gd-5H]^-$: 1020.9; $[1134.1+Gd-5H]^-$: 1287.1).

Synthesis of IRDye-DSPE

IRDye-DSPE was synthesized by conjugating IRDye 800CW NHS ester to DSPE.[33] IRDye 800CW NHS ester powder (2.6 mg) in a glass vial was dissolved with 0.9 ml DMSO on ice and mixed with 1.92 ml of 3% TEA/$CHCl_3$ containing 1.9 mg DSPE (molar ratio, 1:1.15). The vial was kept in dark at 35°C for 20 hr with constant shaking. Then, the mixture was flushed with nitrogen gas to near dryness and then freeze-dried. The dried product was dissolved with 1 ml water, centrifuged at 5,000 g for 1 min. The residual pellets were washed with another1 ml water and centrifuged again. Each 1 ml of the combined supernatants was loaded on a FPLC HiTrap column and eluted with water. The 0.4-ml eluent fractions with color were analyzed by thin layer chromatography (Silica gel 60 F254, plastic sheet, EM Science, NJ) with a mobile phase of MeOH and the absorbance at 778 nm was measured for determination of the dye content. Then the fractions were freeze-dried and stored in the dark at -20°C until needed. The yield of IRDye-DSPE in the first 4 fractions

was approximately 42% of IRDye, assuming the same molar absorption coefficient with IRDye and IRDye-DSPE.

The IRDye-DSPE product was also verified by MALDI-TOF MS assay using DHB matrix (IRDye 800CW: m/z in positive mode. M^+: 1002.2; IRDye-DSPE: m/z in positive mode. $[1002.2+DSPE-H_2O-C_{17}H_{35}CO]^+$: 1467.1).

Preparation of Gd-liposomes

Gadolinium-liposomes (Gd-liposomes), composed of DSPC/cholesterol/Gd-DOTA-DSPE/DOTA-DSPE (molar ratio: 39:35:25:1) containing trace amount of ^{153}Gd and having ammonium sulfate/pH gradient, were prepared by lipid film hydration and extrusion.[18] Briefly, the lipid components were mixed and dissolved with chloroform in a round flask and dried by rotary evaporation under reduced pressure. The formed lipid film was hydrated with 300 mM ammonium sulfate, pH 5.1 to give a concentration of 60 mM total lipids, incubated at 56°C, and vortexed vigorously. The formed milky suspension was sequentially extruded through Whatman Nuclepore polycarbonate membrane filters with different pore sizes (two passes for 2 μm, 1 μm, 400 nm, and 200 nm pore sizes, and six passes for 100 nm pore size) at 56°C (Lipex Extruder; Northern Lipids, Vancouver, British Columbia, Canada). Radioactivity of ^{153}Gd in the extruded liposomes was measured for calculation of lipid recovery. Particle sizes of the liposomes were measured with a DynaPro dynamic light scattering system (Wyatt Technology, CA). Endotoxin levels assayed with limulus amebocyte lysate (LAL) Pyrotell (Associates of Cape Cod Inc., E. Falmouth, MA) were < 12.5 EU/ml. There were no bacteria or fungus growth during 14-day culture.

Post-insertion of IRDye-DSPE into pre-manufactured Gd-liposomes

The synthesized IRDye-DSPE was incorporated into pre-manufactured Gd-liposomes using the reported post-insertion method of phospholipid conjugates.[34-36] The pre-manufactured Gd-liposomes (0.16 ml) were mixed with 0.8 ml of IRDye-DSPE in water (molar ratio of IRDye-DSPE to total lipids: 0.05%) and incubated at 60°C in dark with intermittent vortexing for 1 hr. The mixture was cooled to room temperature and centrifuged at 244,000 *g* for 45 min at 4°C. After the supernatant was aspirated, the pellets were resuspended in 100 mM ammonium sulfate and centrifuged again. The pellets were resuspended in 300 mM ammonium sulfate and stored at 4°C. The absorbance of supernatants at 780 nm was measured to obtain the efficiency of IRDye-DSPE insertion to liposomes.

Post-loading of ^{99m}Tc into liposomes and in vitro stability of ^{99m}Tc-liposomes

The prepared liposomes were labeled with ^{99m}Tc using the method developed in our laboratory with slight modification.[17,37] In brief, 3.5 μl BMEDA and 50 mg sodium glucoheptonate were dissolved with 5 ml nitrogen gas flushed saline, and added with 60 μl of 15 mg/ml $SnCl_2$ in 0.12 M HCl/saline. Then 50 mM NaOH was added to adjust the pH to 7 - 8. One ml aliquot of the mixture was mixed with 0.2 ml (740 MBq (20 mCi)) of sodium ^{99m}Tc-pertechnetate (GE Healthcare) and incubated at 25°C for 20 min to form ^{99m}Tc(V)-BMEDA complex. Then, 0.5 ml of liposomes (total lipids: 60 mM for Gd-liposomes, 30 mM for IRDye-Gd-liposomes) was buffer exchanged by loading on a PD-10 desalting column and elution with phosphate buffered saline (PBS), pH 7.4, then mixed with the ^{99m}Tc(V)-BMEDA complex and incubated at 39°C for 1 hr. The ^{99m}Tc labeled liposomes were purified using the desalting column chromatography. Radiolabeling efficiency was calculated as the ratio of radioactivities of ^{99m}Tc-liposomes post- and pre-purification measured with a dose calibrator (Atomlab 100; Biodex Medical Systems, Shirley, New York).

An aliquot of purified ^{99m}Tc-liposomes was 1:1 V/V diluted with fetal bovine serum (FBS) and incubated at 37°C and the remaining ^{99m}Tc-liposomes were stored at 25°C. The ^{99m}Tc-labeling stability of ^{99m}Tc-liposomes at different times in these two conditions was measured by a GFC-04-500 gel spin microcolumn separation method as described previously.[17,38]

Radiolabeling of Gd-liposomes with ^{64}Cu

Sixty μl of $^{64}CuCl_2$ stock solution (~78 MBq (2.11 mCi)) was diluted with 200 μl 100 mM sodium acetate buffer, pH 6.5. Gd-liposomes (0.5 ml) was loaded on a PD-10 column and eluted with 100 mM acetate buffer, pH 6.5. The collected liposome fraction (1.7 ml) was mixed with the ^{64}Cu radiotracer and incubated at 43°C for 2 hr. Then the mixture was purified using another PD-10 column pre-equilibrated with saline. The percentage of ^{64}Cu associated with Gd-liposomes was determined as the ratio of radioactivities of liposomes post- and pre-purification. For stability evaluation, an aliquot of purified ^{64}Cu-liposomes was 1:1 (V/V) diluted with FBS and incubated at 37°C. Another aliquot of the purified ^{64}Cu-liposomes was stored at room temperature (25°C). Twenty four hr later, the ^{64}Cu-liposomes were purified using the above mentioned column separation method for in vitro stability evaluation of ^{99m}Tc-liposomes.

Post-loading of doxorubicin into Gd-liposomes

One ml of pre-manufactured Gd-liposomes were loaded on a PD-10 column and eluted with saline. The liposomes in saline and doxorubicin hydrochloride in saline were preheated at 43°C, 50°C, 56°C or 60°C, respectively, then mixed together at different drug/lipid ratios and final liposome concentrations. After 30 min, 1 hr, 1.5 hr and 2 hr of incubation with intermittent shaking, a 100 μl aliquot of the mixture was purified by loading on a pre-equilibrated 1-ml Sephadex microcolumn and eluted with saline. The collected liposome fractions, together with the unpurified samples as standards, were digested by 1:2 (V/V) dilution with 2-propanol containing 100 mM HCl (120/1 (V/V) of 2-propanol/12 M HCl). The absorbance at 480 nm was measured for quantification of doxorubicin. Doxorubicin loading efficiency was calculated as the ratio of doxorubicin in doxorubicin-liposomes to the unpurified mixture. The stability of purified doxorubicin-liposomes in saline or in 50% FBS/saline following incubation was also determined by a GFC-04-500 gel spin microcolumn separation method as described previously.[17,38]

Animal model

Animal experiments were preformed in accordance with the NIH Animal Use Guidelines and with approval of local Institutional Animal Care Committee. A human SCCHN xenograft model in nude rats previously established [39] was used for all the imaging experiments. All the animal handling procedures, including cell inoculation, drug injection and in vivo imaging were conducted while the animals were anesthetized with 1-3% isoflurane (Vedco, St. Joseph, MO) in 100% oxygen using an anesthesia inhalation unit (Bickford, Wales Center, NY). SCC-4 cell line(ATCC, Manassas, VA) was cultured in DMEM supplemented with 10% FBS, 100 U/ml penicillin, 100 mg/ml streptomycin and 10 mM HEPES buffer solution (Invitrogen, Grand Island, NY) at 37°C with 5% CO_2. The cells at 80-90% confluence were collected and made into a cell suspension in saline. Male *rnu/rnu* athymic nude rats (Harlan, Indianapolis, IN) at age 4–5 weeks (75–100 g) were inoculated subcutaneously with 5 million of SCC-4 tumor cells in 0.20 ml of saline on the dorsum at the level of the scapulae. The tumor was usually palpable 7 days post tumor cell inoculation. The tumor volume (*V*) was determined by measuring the length (*l*), width (*w*) and depth (*d*) of each tumor with a digital caliper and using an ellipsoid volume formula,

$V=(\pi/6)lwd$. Animals were used for the study at 15 to 25 days after tumor cell inoculation, with an average tumor volume of 1.9 ± 1.1 cm^3.

MR imaging

The Gd-liposomes (0.6 ml with 52 mM total lipids) was purified by PD10 column separation using PBS, pH 7.4 as eluant and diluted to 7 mM of total lipids. Eight nude rats bearing SCCHN tumors were each intratumorally infused with the Gd-liposomes at a volume of 15% of tumor volume and a rate of 0.5 ml/min using a micro-infusion pump (KD Scientific, Holliston, Massachusetts). Pre- and post-infusion of the Gd-liposomes, MR images were acquired with a 7T Bruker PharmaScan® MR scanner (Bruker BioSpin, Ettlingen, Germany) with 7-Tesla/16-cm horizontal bore and a 37-Gauss/cm gradient insert (Billerica, MA). Each rat was positioned so that the entire tumor could fit into the surface coil, and covered with a warm water blanket to maintain the body temperature. Prior to Gd-liposome infusion, high resolution T2- and T1-weighted MR imaging of the tumor was performed. T2-weighted MR images were acquired using rapid acquisition with relaxation enhancement (RARE) pulse sequence with 2D acquisition mode (matrix size: 128 × 128; voxel size: 0.20 × 0.20 mm^2 with 0.52 mm slice thickness; TE = 33.2 ms; TR = 3500 ms; ETL = 8; number of average = 12). T1-weighted MR images were acquired using fast low angle shot (FLASH) pulse sequence with 3D acquisition mode (matrix size: 256 × 256; voxel size: 0.088 × 0.088 × 0.088 mm^3; TE = 3.14 ms; TR = 22.17 ms; flip angle = 45°; number of average = 6). The number of slices of each MR image acquisition was selected to ensure that the entire tumor had been included with each MR image acquisition. Repeated T1-weighted MR imaging with the same imaging parameters and field of view was performed post-infusion of Gd-liposomes to obtain liposome intratumoral micro-distribution.

NIR fluorescent imaging

The freshly prepared IRDye-Gd-liposomes were diluted to 7 mM of total lipids. Four nude rats bearing the SCCHN tumor were each intratumorally infused with the liposomes using the same infusion conditions described above. For comparison, the free IRDye dissolved in PBS, pH 7.4 at the same dye concentration as the IRDye-Gd-liposomes was intratumorally infused into another 4 SCCHN tumor bearing rats. In vivo NIR images of the animals in the supine position during the infusion, and at 2 hr and 24 hr post-infusion were obtained with a Xenogen IVIS Spectrum system using Living Imaging software (Caliper, Xenogen, Alameda, CA). The NIR images (subject size, 3.5; emission filter, 800 nm; excitation filter, 745 nm; exposure time, 1 s; F number, 2; binning factor, 8) were fused with corresponding photographic images (FOV: 13.1 cm; exposure time: 0.2 s; binning factor: 4) for display. At 24 hr after image acquisition, the rats were euthanized by cervical dislocation under deep anesthesia sedation. The NIR images of dissected tumor and other major organs in the body cavity were also acquired.

Gamma camera imaging

^{99m}Tc labeled Gd-liposomes (222 MBq/ml (6.0 mCi/ml), 7 mM total lipids) was intratumorally infused into 4 SCCHN tumor bearing nude rats. Planar gamma camera images were acquired at various time points with each rat in prone position using a micro-SPECT/CT scanner (XSPECT, Gamma Medica, CA) equipped with parallel hole collimators. A vial of known amount of ^{99m}Tc was located in the image field of view as a reference standard. The acquisition time was 1 min at baseline, 2 hr and 4 hr post-infusion, 5 min at 24 hr, and 10 minutes at 44 hr. The percent of injected dose (%ID) of ^{99m}Tc associated with the tumor was quantified by drawing regions of interest and comparing with the ^{99m}Tc standard measured together with the rat.

Micro-PET imaging

Two SCCHN tumor bearing nude rats were intratumorally infused with 15% tumor volume of freshly purified ^{64}Cu labeled liposomes described above. PET images were acquired immediately and 24 hr post-injection of ^{64}Cu-liposomes with a microPET R4 scanner (Siemens Medical Systems), while the rat was positioned to align the tumor in the center of the field of view in both axial and longitudinal directions.

The PET images were reconstructed using 2D ordered-subset expectation maximization (OSEM) into single-frame images and 10 s/frame dynamic images with small-animal PET manager software (Concorde MicroSystems) (matrix size: 128 × 128 × 63; voxel size: 0.85 × 0.85 mm^2; slice thickness: 1.20 mm). The PET images were displayed and analyzed with IDL-based ASIPro® software (Concorde MicroSystems).

RESULTS

Preparation of liposomes containing synthesized functional components

DOTA-DSPE and Gd-DOTA-DSPE were prepared by one-step syntheses and purified with high yields (> 90%) using more simple and convenient procedures than previously reported.[21,22] IRDye-DSPE was also effectively synthesized. Some of the IRDye-DSPE was not recovered due to the incomplete separation from free dye during the gel filtration chromatography, leading to the yield of pure IRDye-DSPE being about 40%.

The particle sizes of prepared Gd-liposomes were 112.9 ± 1.5 nm of diameter with 18.2% polydispersity. The Gd-liposome preparation described herein also had a high recovery of Gd-DOTA-DSPE as obtained by ^{153}Gd radioactivity measurement (nearly 90%) and the particle sizes did not vary during 6 months storage at 4°C, indicating the effective integration of Gd-DOTA-DSPE with other lipid components to form stable liposomes. Cautious extrusion through a series of filters with decreasing pore sizes should be preformed to avoid the loss of lipids retained on filters, which may contribute to the reported low recovery of Gd-DOTA-DSPE.[21] IRDye-DSPE (0.05% of total lipids) could be post-inserted into preformed liposomes at high efficiencies (> 95%) without a significant change in liposome particle size.

Radiolabeling of preformed Gd-liposomes

The ^{99m}Tc labeling efficiencies of Gd-liposomes and IRDye-Gd-liposomes were in a range of 58-89%, similar to that of liposomes comprised of DSPC and cholesterol only.[38] The ^{99m}Tc-Gd-liposomes were stable both in PBS, pH 7.4 and in 50% FBS/PBS; more than 79% of ^{99m}Tc still associated with liposomes at 72 hr post-incubation (Figure 3). The presence of DOTA-DSPE in the liposome formulation slightly decreased the ^{99m}Tc labeling stability in PBS, pH 7.4 as compared with DSPC/cholesterol liposomes.[38] However, the ^{99m}Tc labeling stabilities of liposomes with or without DOTA-DSPE component were similar in 50% FBS/PBS.

The labeling efficiency of Gd-liposomes containing 1 mole % DOTA-DSPE with ^{64}Cu tracer was 96.4 ± 2.9% (n = 2). After 24 hr in PBS, pH 7.4 at 25°C or in 50% FBS/PBS at 37°C, the percentage of ^{64}Cu associated with liposomes were 96.6% and 94.4%, respectively, indicating that the addition of only 1% of the DOTA-DSPE component was reliable for conjugating and anchoring ^{64}Cu stably on the liposome surface.

Doxorubicin loading of preformed Gd-liposomes

Doxorubicin is a well established weak alkalic anticancer agent for the treatment of a broad range of solid tumors. The remote loading of doxorubicin into liposomes has remarkable

advantages of high drug to lipid ratio, as well as improved drug cancer targeting for enhanced cancer therapy and reduced toxicity.[40,41] In our study, highly efficient encapsulation of doxorubicin into ammonium/pH gradient DSPC/cholesterol liposomes was achieved. Under conditions of changing the liposome medium to saline and heating the mixture of doxorubicin and liposomes (drug/lipid ratio, W/W 1:5, 16 mM of total lipids) at 60°C for 40 min, a drug loading of > 90% was achieved. However, the remote loading of doxorubicin into the ammonium sulfate/pH gradient Gd-liposomes was relatively more difficult. After incubated at 43°C for 2 hr, the loading of doxorubicin into Gd-liposomes was insignificant. Incubation at 56 -60°C tended to cause the aggregation of liposomes at drug/lipid ratios (W/W) of 1/10 - 1/4 and total lipid concentrations of 5 - 9 mM, a low doxorubicin loading efficiency (< 32% after 1 hr incubation); whereas when the drug/lipid ratio was reduced to 1/15 and the mixture was diluted to 2.5 mM of total lipids, the loading efficiency could be improved to 56% but the absolute drug loading amount was lower. The optimized loading conditions were 1/10 of a drug/lipid ratio, 5 mM of total lipids in saline and incubation at 50°C for 1.5 hr, which led to a 65% loading efficiency, corresponding to 6.5/100 of doxorubicin/lipids in purified liposomes. Simply increasing of drug/lipid ratio, and liposome concentration or extending the incubation time could not improve the drug loading amount.

The particle sizes of purified doxorubicin-Gd-liposomes were 131.1 ± 3.8 nm. The particle sizes of initial Gd-liposomes were 112.9 ± 1.5 nm. The purified doxorubicin-liposomes were stable at 4°C for weeks without significant drug leakage observed by desalting column separation. The concentration of doxorubicin-Gd-liposomes can be adjusted with centrifugation and resuspension. Although the doxorubicin drug/lipid ratio was lower than that of current doxorubicin-liposome formulations, it is expected that the doxorubicin dose would be high enough for cancer therapy, especially in the situation of direct intratumoral administration.

MR imaging of SCCHN tumor xenografts in nude rats with intratumoral infusion of Gd-liposomes

The typical T2- and T1-weighted MR images of SCCHN tumor pre- and post-Gd-liposome infusion are shown in Figure 4. The heterogeneous microstructure of tumor could be visualized by both the T2- and T1-weighted MR images. Post-intratumoral infusion, the T1-weighted MR images clearly showed the region of Gd-liposome distribution in the tumor (Figure 4). Thus, contrast enhanced MR imaging could enable the non-invasive evaluation of Gd-liposome distribution in the tumor, guide the treatment planning for local drug administration and predict the cancer therapy response.

Contrast enhanced MR imaging has advantages of providing anatomic function and affording high resolution of intratumoral microdistribution of liposomes compared to nuclear imaging. The disadvantage of contrast enhanced MR imaging is that a relatively high concentration of Gd has to be present in the liposome formulation to surmount its low intrinsic sensitivity. Accordingly, nuclear imaging provides high sensitivity and better quantification.

NIR fluorescent imaging of SCCHN tumor xenografted nude rats with intratumoral infusion of IRDye-Gd-liposomes

The series of NIR fluorescent images acquired in a dynamic mode showed the gradual dispersion of IRDye-Gd-liposomes or free IRDye inside the tumor during the intratumoral infusion. The fluorescent intensities (radiant efficiency, $p/sec/cm^2/sr/(\mu W/cm^2)$) of IRDye-liposome group measured at 24 hr post-infusion were lower than that measured at 1 min, whereas that measured at 2 hr post-infusion were significantly stronger, which is projected

to be caused by the local diffusion and stable intratumoral retention of IRDye-liposomes. On the contrary, the fluorescent intensities at the tumor site of free IRDye group were decreased significantly at 2 hr post-injection (Figure 5A), which is coincident with the rapid clearance of IDye 800CW in the circulation system (half life in Sprague-Dawley rats: 35.7 min post intravenous injection, 235.6 min post-intradermal injection.[42] The average relative fluorescent intensities normalized to that at 1 min post-injection are shown in Figure 5B. These results reflected the high sensitivity of IRDye-DSPE tracer to identify the local spatial and temporal distribution and retention of the liposomes, indicating it is feasible for the monitoring of IRDye-liposomes with NIR fluorescence tomography technique.

The NIR images of dissected tumor and normal organs revealed that the liposomes injected at 15% of tumor volume might not cover the entire tumor, and the cleared liposomes showed insignificant accumulation of trace dye component in liver, spleen, kidneys, lung and heart (Figure 5C). Multiple injection locations and higher injection volume of liposomes will be necessary for more effective delivery of drug inside the tumor.

Gamma camera imaging of SCCHN xenografted nude rats with intratumoral infusion of ^{99m}Tc-Gd-liposomes

Planar gamma camera images were acquired at different times for monitoring the in vivo distribution of 99mTc-Gd-liposomes post-intratumoral injection in the SCCHN xenografted nude rats. These images revealed that a high percentage of injected dose (ID) was retained inside the tumor during the 44 hr experimental period. The cleared radioactivity from tumor was excreted rapidly and had no significant accumulation in any vital organ (Figure 6), similar to our previous observations with liposomes comprised of DSPC/cholesterol and having ammonium sulfate/pH gradient but without functional lipid derivative.[27] The quantification of ^{99m}Tc-Gd-liposomes retained in the tumor at various times post-injection was derived from region of interest analysis of these gamma camera images and indicated their high intratumoral retention.

Micro-PET imaging of SCCHN xenografts with intratumoral infusion of ^{64}Cu-Gd-liposomes

Micro-PET images were acquired at 24 hr post-intratumoral infusion of ^{64}Cu-Gd-liposomes (Figure 7). The 3D tomographic and projection images clearly showed the local retention and micro-distribution of radioactivity in the tumor.

DISCUSSION

Liposomal drug delivery systems have shown promising applications for cancer treatment with chemotherapeutic drugs, genetic agents and therapeutic radionuclides.[14] The non-invasive multi-modality imaging of theranostics will enable optimal real time monitoring of both the systemic and micro-distribution of delivered therapeutic agents taking advantage of their synergistic effect to guide the adjustable personalized scheme of drug administration and therapy with an accurate prediction of treatment response. To achieve this goal, we designed and investigated a liposomal drug delivery system, which integrated MR, NIR fluorescent and SPECT or PET multi-modality imaging, as well as with the carriage of chemotherapeutic drug and/or therapeutic radionuclides for personalized cancer theranostics.

As shown in Figure 1, liposomes are lipid nanoparticles comprised of various kinds of lipids, including cholesterol or its similar chemicals, which form a lipid double membrane spherical structure; while enclosing a segregated aqueous space. This unique structural feature possessed by liposomes has long been recognized as an ideal drug delivery vehicle for in vivo controlled drug release, improved efficacy, or lower toxicity. The drug molecules can be encapsulated in the inner aqueous space, or if lipophilic drug molecules, can be

embedded in the lipid double membrane. Meanwhile, through conjugation to a lipid chain, various drug molecules can also be linked to the membrane surface either during liposome manufacture or via post-insertion. Correspondingly, a broad spectrum of imaging or targeting groups can also be added to liposomes based on the same mechanisms. As with liposomes, other nanoparticles may also be modified to be multifunctionalized.[10] Comparably, liposomes excel over other nanoparticle systems in efficient and high concentration drug loading, universally applicable methods of imaging and targeting modifications, as well as the proven clinical success in human disease treatment.[11-17]

The liposomes, composed of Gd-DOTA-DSPE/DOTA-DSPE/DSPC/cholesterol (molar ratio: 25:1:39:35) and having ammonium sulfate/pH gradient, were prepared by lipid film hydration and extrusion. IRDye-DSPE tracer can be effectively incorporated into liposomes by post-insertion method. By using the ammonium sulfate/pH gradient between liposome interior and exterior, the pre-manufactured liposomes can also be radiolabeled with the most widely used diagnostic radionuclide, ^{99m}Tc, as well as its chemical mimic, therapeutic radionuclides, ^{186}Re/^{188}Re.[18,20] The introduction of a low percentage of DOTA-DSPE allows for the liposome surface labeling with PET imaging radionuclide, ^{64}Cu, or other appropriate radionuclides with high labeling stabilities. The chemotherapeutic agent, doxorubicin could be effectively post-loaded into the pre-manufactured liposomes. A weight ratio of doxorubicin to total lipids, 6.1/100, corresponding to 1.9 mg of doxorubicin in a liposome suspension of 40 mM of total lipids, was achieved under the optimized conditions. The doxorubicin-liposomes were stable when stored at 4°C. These results indicated the successful establishment of a non-invasive in vivo multimodality functional imaging and therapeutic liposomal drug delivery system for cancer theranostics.

In the preliminary in vivo multimodality imaging evaluation of the multifunctional liposomal drug delivery system, we investigated the locoregional retention and biodistribution of the Gd-liposomes, IRDye-liposomes, ^{99m}Tc labeled liposomes, or ^{64}Cu labeled liposomes after intratumoral infusion into SCCHN xenografts in nude rats using MR, NIR fluorescent, planar gamma and PET imaging modalities, respectively. MR imaging provided a 3D high resolution intratumoral micro-distribution of the liposomes, which will be important for the prediction of cancer therapy response. Both the in vivo NIR fluorescent and nuclear images clearly showed the retention and distribution of liposomes inside the tumor. The NIR fluorescent signal emitted by the trace IRDye moiety had high sensitivity and was convenient for detecting the locoregional retention and systemic distribution at superficial areas of the body. Nuclear images can accurately measure the quantitative biodistribution of administrated radioactivity in vivo. Our radiolabeling of liposomes with ^{99m}Tc and ^{64}Cu used distinct mechanisms. ^{99m}Tc was encapsulated into the inner aqueous space, whereas ^{64}Cu was chelated with the DOTA group on the bilayer membrane surface. Their stabilities represented the specific transmembrane permeability shown by ^{99m}Tc and lipid bilayer integrity by ^{64}Cu. The in vivo imaging results of ^{99m}Tc- and ^{64}Cu-labeled Gd-liposomes verified the effectiveness of delivery of radionuclides by liposome carriers, which could be highly retained inside the tumor with a micro-heterogeneous intratumoral distribution. The resolution of nuclear images was lower than MR images; however, nuclear imaging possesses better quantification feature.

The biological behavior of the liposomes obtained by each imaging modality may be interfered by others in the same multifunctional nanoparticle. Investigation of the pharmacokinetics with noninvasive imaging techniques has great potential for the optimal design and application of multifunctional nanoparticles. In this study, we integrated non-interfering mechanisms for constructing the multifunctional liposomes with different biocompatible functional constitutes, avoiding the pitfalls of low yield and low stability typically observed with multi-step constructions of multifunctional nanoparticles.

Some other methods of enabling MR contrast have been demonstrated for monitoring of liposomal drug delivery.[43-46] For MR imaging, lipidized or lipophilic Gd agent can be incorporated in the lipid bilayers.[45,47-49] Hydrophilic manganese (Mn) ions or Gd-DTPA complexes have been encapsulated in the liposome internal aqueous space to study the release of drug molecules from liposomes by a triggering mechanism, such as hyperthermia, and imaged by T1-weighted MR.[32,43,44,50-52] However, the toxicity of Mn ions limits its clinical application.[53] The chelation of Gd with macrocyclic ligand, DOTA, has higher thermodynamic and kinetic stability than with the linear ligand, DTPA.[54] Passive encapsulation of Gd-DTPA into liposomes results in a low concentration of Gd in the liposome suspension; and consequently, a relatively low MR signal sensitivity. The use of Gd-DOTA-DSPE can avoid these shortcomings. The high percentage of Gd-DOTA-DSPE component presented in our liposome formulation produced strong T1-weighted MR signal indicating the micro-distribution of liposomes following intratumoral infusion, which can lead to accurately predicting the tumor response of local liposomal chemotherapy or radiotherapy.

The lipidized macrocyclic ligand, DOTA-DSPE, was incorporated in liposomes for chelation of ^{64}Cu. Although radiolabeling of liposomes with ^{64}Cu can be realized via a post-loading method [55] or conjugation with maleimide lipid of ^{64}Cu pre-labeled bifunctional chelators with thiol group,[56,57] our method represents an option for convenient and stable ^{64}Cu-liposome radiolabeling. Notably, our liposome drug delivery system has the capability of being radiolabeled with therapeutic radionuclides for radionuclide therapy, which when compared with most chemotherapy and gene therapy agents, has the advantages of not requiring as close of a proximity of the liposomes to the cell surface and intracellular uptake of the radionuclides. In spite of the therapeutic potential of ^{186}Re/^{188}Re encapsulated Gd-liposomes, the DOTA-DSPE component is also potentially suitable for the labeling of liposomes with other beta emitting therapeutic radionuclides of rare earth elements as they share similar chemical properties, such as samarium-153(^{153}Sm) and lutetium-177 (^{177}Lu),[58] and also copper-67 (^{67}Cu) ($T_{1/2}$ = 61.8 hr).[59,60]

Other approaches have been used to construct multifunctional and theranostic liposomes.[7-9] Some of these approaches can be combined with ours to further improve the function and application potential of liposomes. For example, our radiolabeling method could be useful for investigating the systemic pharmacokinetics of other types of liposomes. We will investigate the possibility of extended functionalization, such as active targeting modification and the image guided therapeutic potential of our multifunctional liposome drug delivery system in future studies.

CONCLUSION

We developed a multifunctional liposome drug delivery system containing Gd-DOTA-DSPE, DOTA-DSPE and having ammonium sulfate/pH gradient. These multifunctional liposomes can be labeled with NIR fluorescent tracer, IRDye-DSPE by post-insertion method and radiolabeled with radioisotopes for nuclear imaging, such as ^{99m}Tc by post-loading, or ^{64}Cu by conjugation to DOTA moiety on the liposome surface. The representative chemotherapeutic agent, doxorubicin can also be effectively remote loaded into the multifunctional liposomes. The local retention and systemic biodistribution data with a tumor xenograft model of SCCHN demonstrated that these multifunctional liposomes are promising drug carriers, enabling non-invasive multimodality imaging of their in vivo behavior with MR, NIR fluorescence, SPECT or PET imaging techniques. In addition, these multifunctional liposomes have potential for the accurate monitoring and guidance the in vivo delivery of liposomal chemotherapeutic drugs or therapeutic radionuclides by taking advantages of various available non-invasive imaging modalities.

Acknowledgments

This study was financially supported by NIH/NCI grant, R01 CA131039. The MR and PET imaging study cost was supported by CTSA grant, UL1 RR025767. In vivo near infrared fluorescent images were generated in the Core Optical Imaging Facility, University of Texas Health Science Center at San Antonio.

REFERENCES

(1). Khullar O, Frangioni JV, Grinstaff M, Colson YL. Image-guided sentinel lymph node mapping and nanotechnology-based nodal treatment in lung cancer using invisible near-infrared fluorescent light. Semin. Thorac. Cardiovasc. Surg. 2009; 21:309–315. [PubMed: 20226343]

(2). Troyan SL, Kianzad V, Gibbs-Strauss SL, Gioux S, Matsui A, Oketokoun R, Ngo L, Khamene A, Azar F, Frangioni JV. The FLARE intraoperative near-infrared fluorescence imaging system: a first-in-human clinical trial in breast cancer sentinel lymph node mapping. Ann. Surg. Oncol. 2009; 16:2943–2952. [PubMed: 19582506]

(3). Moser E, Stadlbauer A, Windischberger C, Quick HH, Ladd ME. Magnetic resonance imaging methodology. Eur. J. Nucl. Med. Mol. Imaging. 2009; 36(Suppl 1):S30–S41. [PubMed: 19104805]

(4). Lanza GM, Winter PM, Caruthers SD, Morawski AM, Schmieder AH, Crowder KC, Wickline SA. Magnetic resonance molecular imaging with nanoparticles. J. Nucl. Cardiol. 2004; 11:733–743. [PubMed: 15592197]

(5). Blasberg RG, Gelovani J. Molecular-genetic imaging: A nuclear medicine–based perspective. Mol. Imaging. 2002; 1:280–300. [PubMed: 12920854]

(6). Margolis DJA, Hoffman JM, Herfkens RJ, Jeffrey RB, Quon A, Gambhir SS. Molecular imaging techniques in body imaging. Radiology. 2007; 245:333–356. [PubMed: 17940297]

(7). Koning GA, Krijger GC. Targeted multifunctional lipid-based nanocarriers for image-guided drug delivery. Anticancer Agents Med. Chem. 2007; 7:425–440. [PubMed: 17630918]

(8). Jennings LE, Long NJ. 'Two is better than one' — probes for dual-modality molecular imaging. Chem. Commun. (Camb.). 2009; 24:3511–3524. [PubMed: 19521594]

(9). Martí-Bonmatí L, Sopena R, Bartumeus P, Sopena P. Multimodality imaging techniques. Contrast Media Mol. Imaging. 2010; 5:180–189. [PubMed: 20812286]

(10). Louie A. Multimodality imaging probes: design and challenges. Chem. Rev. 2010; 110:3146–3195. [PubMed: 20225900]

(11). Buse J, El-Aneed A. Properties, engineering and applications of lipid-based nanoparticle drug-delivery systems: current research and advances. Nanomedicine. 2010; 5:1237–1260. [PubMed: 21039200]

(12). Lammers T, Kiessling F, Hennink WE, Storm G. Nanotheranostics and image-guided drug delivery: current concepts and future directions. Mol. Pharm. 2010; 7:1899–1912. [PubMed: 20822168]

(13). Gabizon, A. Applications of liposomal drug delivery systems to cancer therapy. In: Amiji, MM., editor. Nanotechnology for Cancer Therapy. CRC Press; Boca Raton: 2007. p. 595-611.

(14). Elbayoumi TA, Torchilin VP. Current trends in liposome research. Methods Mol. Biol. 2010; 605:1–27. [PubMed: 20072870]

(15). Farokhzad O, Langer R. Nanomedicine: developing smarter therapeutic and diagnostic modalities. Adv. Drug Deliv. Rev. 2006; 58:1456–1459. [PubMed: 17070960]

(16). Puri A, Loomis K, Smith B, Lee JH, Yavlovich A, Heldman E, Blumenthal R. Lipid-based nanoparticles as pharmaceutical drug carriers: from concepts to clinic. Crit. Rev. Ther. Drug Carrier Syst. 2009; 26:523–580. [PubMed: 20402623]

(17). Bao A, Goins B, Klipper R, Negrete G, Phillips WT. Direct ^{99m}Tc labeling of pegylated liposomal doxorubicin (Doxil) for pharmacokinetic and non-invasive imaging studies. J. Pharmacol. Exp. Ther. 2004; 308:419–425. [PubMed: 14610219]

(18). Bao A, Goins B, Klipper R, Negrete G, Phillips WT. ^{186}Re-liposome labeling using ^{186}Re-SNS/S complexes: in vitro stability, imaging, and biodistribution in rats. J. Nucl. Med. 2003; 44:1992–1999. [PubMed: 14660726]

(19). Cullis PR, Hope MJ, Bally MB, Madden TD, Mayer LD, Fenske DB. Influence of pH gradients on the transbilayer transport of drugs, lipids, peptides and metal ions into large unilamellar vesicles. Biochim. Biophys. Acta. 1997; 1331:187–211. [PubMed: 9325441]

(20). Eckerman, KF.; Endo, A. MIRD: Radionuclide Data and Decay Schemes. 2nd Edition. Society of Nuclear Medicine; Reston, VA: 2008. p. 103(^{64}Cu); 232-233 (^{99m}Tc); 392-393 (^{153}Sm); 415-417 (^{153}Gd); 460-461 (^{177}Lu); 485-486 (^{188}W); 487-488 (^{186}Re); 489-490 (^{188}Re)

(21). Hak S, Sanders HM, Agrawal P, Langereis S, Grüll H, Keizer HM, Arena F, Terreno E, Strijkers GJ, Nicolay K. A high relaxivity Gd(III)DOTA-DSPE-based liposomal contrast agent for magnetic resonance imaging. Eur. J. Pharm. Biopharm. 2009; 72:397–404. [PubMed: 18940253]

(22). Oliver M, Ahmed A, Kamaly N, Perouzel E, Caussin A, Keller M, Herlihy A, Bell J, Miller AD, Jorgensen MR. MAGfect: a novel liposome formulation for MRI labeling and visualization of cells. Org. Biomol. Chem. 2006; 4:3489–3497. [PubMed: 17036144]

(23). Mulder WJM, Strijkers GJ, van Tilborg GAF, Griffioen AW, Nicolay K. Lipid-based nanoparticles for contrast-enhanced MRI and molecular imaging. NMR Biomed. 2006; 19:142–164. [PubMed: 16450332]

(24). Mulder WJ, van der Schaft DW, Hautvast PA, Strijkers GJ, Koning GA, Storm G, Mayo KH, Griffioen AW, Nicolay K. Early in vivo assessment of angiostatic therapy efficacy by molecular MRI. FASEB J. 2007; 21:378–383. [PubMed: 17202248]

(25). Harrington KJ, Rowlinson-Busza G, Syrigos KN, Uster PS, Vile RG, Stewart JS. Pegylated liposomes have potential as vehicles for intratumoral and subcutaneous drug delivery. Clin. Cancer Res. 2000; 6:2528–2537. [PubMed: 10873109]

(26). Bao A, Phillips WT, Goins B, Zheng X, Sabour S, Natarajan M, Woolley FR, Zavaleta C, Otto RA. Potential use of drug carried-liposomes for cancer therapy via direct intratumoral injection. Int. J. Pharm. 2006; 316:162–169. [PubMed: 16580161]

(27). French JT, Goins B, Phillips WT, Saenz M, Li S, Garcia-Rojas X, Otto RA, Bao A. Interventional therapy of head and neck cancer with lipid nanoparticle-carried rhenium-186 radionuclide. J. Vasc. Interven. Radiology. 2010; 21:1271–1279.

(28). Wang SX, Bao A, Herrera SJ, Phillips WT, Goins B, Santoyo C, Miller FR, Otto RA. Intraoperative ^{186}Re-liposome radionuclide therapy in a head and neck squamous cell carcinoma xenograft positive surgical margin model. Clin. Cancer Res. 2008; 14:3975–3983. [PubMed: 18559620]

(29). Hrycushko BA, Ware S, Li S, Bao A. Improved tumour response prediction with equivalent uniform dose in pre-clinical study using direct intratumoural infusion of liposome-encapsulated ^{186}Re radionuclides. Phys. Med. Biol. 2011; 56:5721–5734. [PubMed: 21841210]

(30). Luboldt W, Pinkert J, Matzky C, Wunderlich G, Kotzerke J. Radiopharmaceutical tracking of particles injected into tumors: a model to study clearance kinetics. Curr. Drug Deliv. 2009; 6:255–260. [PubMed: 19604139]

(31). Allard E, Passirani C, Benoit JP. Convection-enhanced delivery of nanocarriers for the treatment of brain tumors. Biomaterials. 2009; 30:2302–2318. [PubMed: 19168213]

(32). Tagami T, Foltz WD, Ernsting MJ, Lee CM, Tannock IF, May JP, Li SD. MRI monitoring of intratumoral drug delivery and prediction of the therapeutic effect with a multifunctional thermosensitive liposome. Biomaterials. 2011; 32:6570–6578. [PubMed: 21641639]

(33). Hermanson, GT. Bioconjugate Techniques. Academic Press – An Imprint of Elsevier; San Diego, CA: 1996. p. 139-140.p. 173-176.

(34). Uster PS, Allen TM, Daniel BE, Mendez CJ, Newman MS, Zhu GZ. Insertion of poly(ethylene glycol) derivatized phospholipid into pre-formed liposomes results in prolonged in vivo circulation time. FEBS Lett. 1996; 386:243–246. [PubMed: 8647291]

(35). Allen TM, Sapra P, Moase E. Use of the post-insertion method for the formation of ligand-coupled liposomes. Cell. Mol. Biol. Lett. 2002; 7:889–894. [PubMed: 12378272]

(36). Moreira JN, Ishida T, Gaspar R, Allen TM. Use of the post-insertion technique to insert peptide ligands into pre-formed stealth liposomes with retention of binding activity and cytotoxicity. Pharm. Res. 2002; 19:265–269. [PubMed: 11934232]

(37). Goins B, Bao A, Phillips WT. Techniques for loading technetium-99m and rhenium-186/188 radionuclides into pre-formed liposomes for diagnostic imaging and radionuclide therapy. Methods Molec. Biol. 2010; 606:469–491. [PubMed: 20013416]

(38). Li S, Goins B, Phillips WT, Bao A. Remote-loading labeling of liposomes with ^{99m}Tc-BMEDA and its stability evaluation: effects of lipid formulation and pH/chemical gradient. J. Liposome Res. 2011; 21:17–27. [PubMed: 20334497]

(39). Bao A, Phillips WT, Goins B, McGuff HS, Zheng X, Woolley FR, Natarajan M, Santoyo C, Miller FR, Otto RA. Setup and characterization of a human head and neck squamous cell carcinoma xenograft model in nude rats. Otolaryngol. Head Neck Surg. 2006; 135:583–587.

(40). Gabizon A, Shmeeda H, Barenholz Y. Pharmacokinetics of pegylated liposomal doxorubicin: Review of animal and human studies. Clin. Pharmacokinet. 2003; 42:419–436. [PubMed: 12739982]

(41). Fenske DB, Cullis PR. Entrapment of small molecules and nucleic acid-based drugs in liposomes. Methods Enzymol. 2005; 391:7–40. [PubMed: 15721372]

(42). Marshall MV, Draney D, Sevick-Muraca EM, Olive DM. Single-dose intravenous toxicity study of IRDye 800CW in Sprague-Dawley rats. Mol. Imaging Biol. 2010; 12:583–594. [PubMed: 20376568]

(43). Krauze MT, Forsayeth J, Park JW, Bankiewicz KS. Real-time imaging and quantification of brain delivery of liposomes. Pharm. Res. 2006; 23:2493–2504. [PubMed: 16972184]

(44). Hossann M, Wang T, Wiggenhorn M, Schmidt R, Zengerle A, Winter G, Eibl H, Peller M, Reiser M, Issels RD, Lindner LH. Size of thermosensitive liposomes influences content release. J. Control. Release. 2010; 147:436–443. [PubMed: 20727921]

(45). Grange C, Geninatti-Crich S, Esposito G, Alberti D, Tei L, Bussolati B, Aime S, Camussi G. Combined delivery and magnetic resonance imaging of neural cell adhesion molecule-targeted doxorubicin-containing liposomes in experimentally induced Kaposi's sarcoma. Cancer Res. 2010; 70:2180–2190. [PubMed: 20215497]

(46). De Smet M, Heijman E, Langereis S, Hijnen NM, Grüll H. Magnetic resonance imaging of high intensity focused ultrasound mediated drug delivery from temperature-sensitive liposomes: an in vivo proof-of-concept study. J. Control. Release. 2011; 150:102–110. [PubMed: 21059375]

(47). Trubetskoy VS, Cannillo JA, Milshtein A, Wolf GL, Torchilin VP. Controlled delivery of Gd-containing liposomes to lymph nodes: surface modification may enhance MRI contrast properties. Magn. Reson. Imaging. 1995; 13:31–37. [PubMed: 7534860]

(48). Weissig VV, Babich J, Torchilin VV. Long-circulating gadolinium-loaded liposomes: potential use for magnetic resonance imaging of the blood pool. Colloids Surf. B Biointerfaces. 2000; 18:293–299. [PubMed: 10915951]

(49). Bui T, Stevenson J, Hoekman J, Zhang S, Maravilla K, Ho RJ. Novel Gd nanoparticles enhance vascular contrast for high-resolution magnetic resonance imaging. PLoS One. 2010; 5:e13082. [PubMed: 20927340]

(50). Viglianti BL, Abraham SA, Michelich CR, Yarmolenko PS, MacFall JR, Bally MB, Dewhirst MW. In vivo monitoring of tissue pharmacokinetics of liposome/drug using MRI: illustration of targeted delivery. Magn. Reson. Med. 2004; 51:1153–1162. [PubMed: 15170835]

(51). Viglianti BL, Ponce AM, Michelich CR, Yu D, Abraham SA, Sanders L, Yarmolenko PS, Schroeder T, MacFall JR, Barboriak DP, Colvin OM, Bally MB, Dewhirst MW. Chemodosimetry of in vivo tumor liposomal drug concentration using MRI. Magn. Reson. Med. 2006; 56:1011–1018. [PubMed: 17029236]

(52). Ponce AM, Viglianti BL, Yu D, Yarmolenko PS, Michelich CR, Woo J, Bally MB, Dewhirst MW. Magnetic resonance imaging of temperature-sensitive liposome release: drug dose painting and antitumor effects. J. Natl. Cancer Inst. 2007; 99:53–63. [PubMed: 17202113]

(53). Silva AC, Lee JH, Aoki I, Koretsky AP. Manganese-enhanced magnetic resonance imaging (MEMRI): methodological and practical considerations. NMR Biomed. 2004; 17:532–543. [PubMed: 15617052]

(54). Morcos SK. Extracellular gadolinium contrast agents: differences in stability. Eur. J. Radiology. 2008; 66:175–179.

(55). Petersen AL, Binderup T, Rasmussen P, Henriksen JR, Elema DR, Kjær A, Andresen TL. ^{64}Cu loaded liposomes as positron emission tomography imaging agents. Biomaterials. 2011; 32:2334–2341. [PubMed: 21216003]

(56). Seo JW, Zhang H, Kukis DL, Meares CF, Ferrara KW. A novel method to label preformed liposomes with ^{64}Cu for positron emission tomography (PET) imaging. Bioconjug. Chem. 2008; 19:2577–2584. [PubMed: 18991368]

(57). Andreozzi E, Seo JW, Ferrara K, Louie A. Novel method to label solid lipid nanoparticles with ^{64}Cu for positron emission tomography imaging. Bioconjug. Chem. 2011; 22:808–818. [PubMed: 21388194]

(58). Uusijärvi H, Bernhardt P, Rösch F, Maecke HR, Forssell-Aronsson E. Electron- and positron-emitting radiolanthanides for therapy: aspects of dosimetry and production. J. Nucl. Med. 2006; 47:807–814. [PubMed: 16644751]

(59). Howell RW, Rao DV, Sastry KS. Macroscopic dosimetry for radioimmunotherapy: nonuniform activity distributions in solid tumours. Med. Phys. 1989; 16:66–74. [PubMed: 2921982]

(60). Novak-Hofer I, Schubiger PA. Copper-67 as a therapeutic nuclide for radioimmunotherapy. Eur. J. Nucl. Med. Mol. Imaging. 2002; 29:821–830. [PubMed: 12029558]

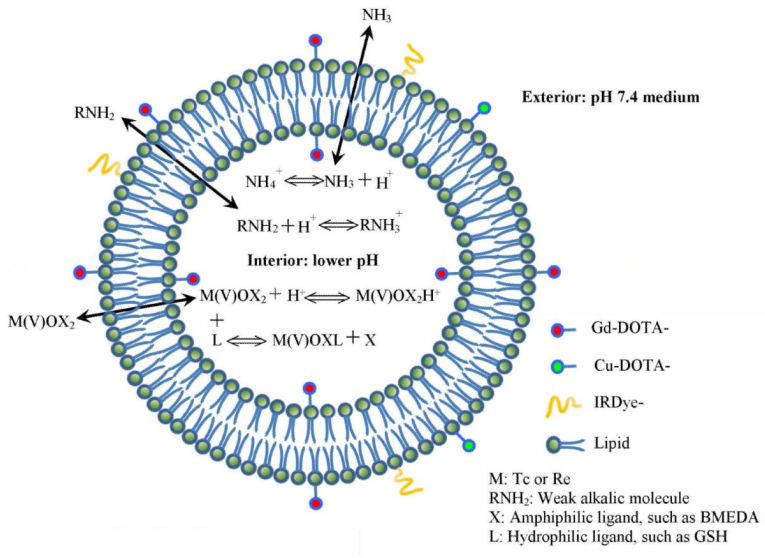

Figure 1.
Schematic diagram of multifunctional liposomes.

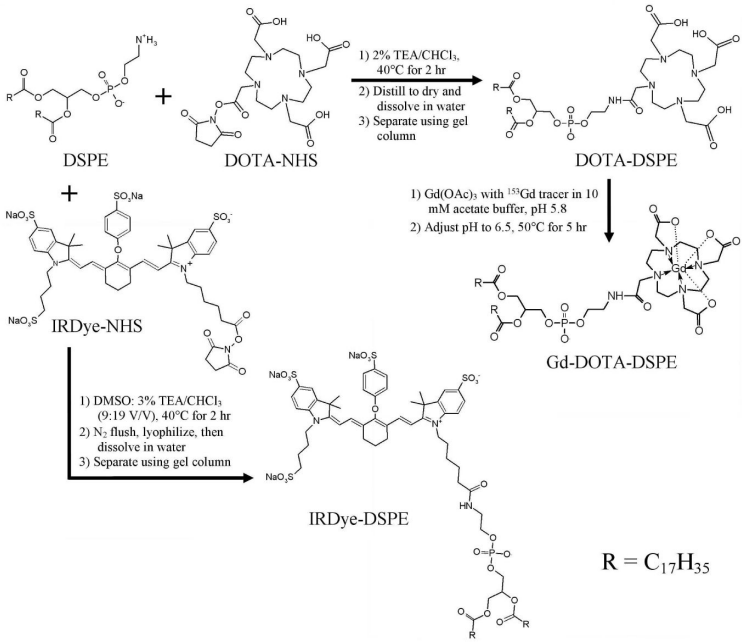

Figure 2.
Synthesis of DOTA-DSPE, Gd-DOTA-DSPE and IRDye-DSPE.[21,22,33]

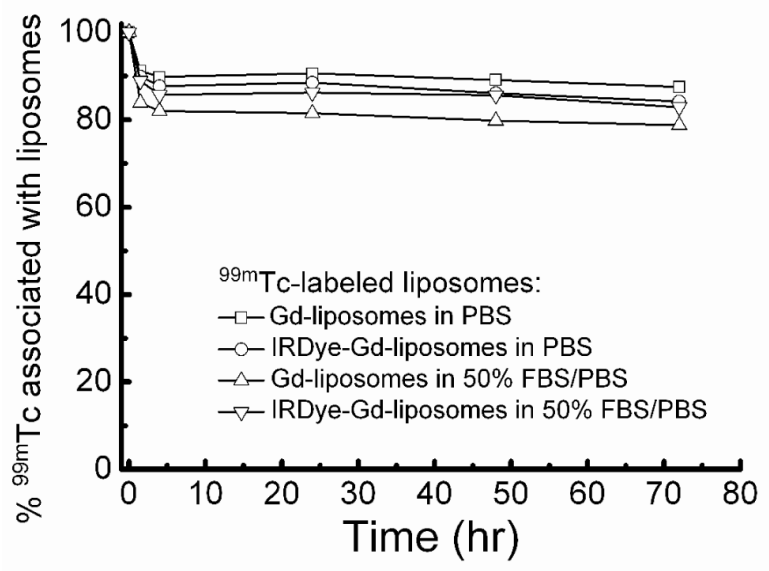

Figure 3.
Percentage of ^{99m}Tc associated with liposomes at different times following incubation in phosphate buffered saline (PBS) and PBS containing 50% fetal bovine serum (FBS).

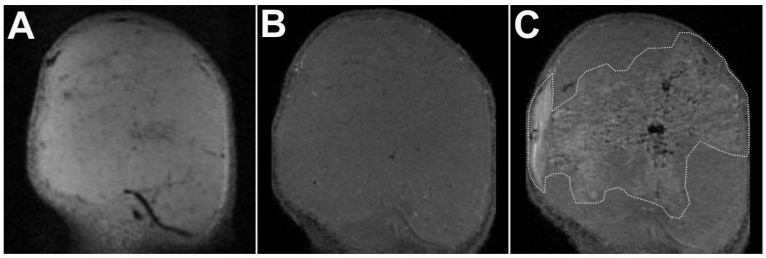

Figure 4.

T2- (**A**) and T1- (**B** and **C**) weighted 7T MR images of SCCHN tumor pre- (**A** and **B**) and post- (**C**) intratumoral infusion of Gd-liposomes using a surface coil. Intratumoral distribution of Gd-liposomes has been circumscribed with dashed white line (**C**).

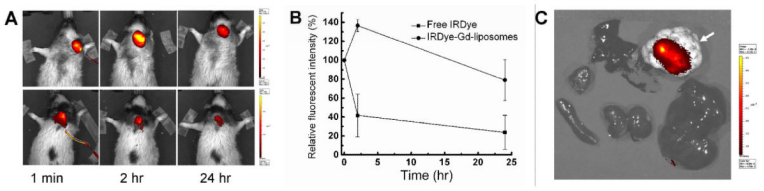

Figure 5.

NIR images and intratumoral fluorescent intensity change of SCCHN xenografted nude rats intratumorally infused with NIR agents. **A**) NIR images at 1 min, 2 hr and 24 hr post intratumoral infusion of IRDye-Gd-liposomes (upper panel) and free IRDye (lower panel); **B**) NIR fluorescent intensity change with time in the tumor area normalized to 1 min post infusion; **C**) NIR images of dissected tumor (white arrow) and normal organs from the rats euthanized 24 hr post intratumoral infusion of IRDye-Gd-liposomes.

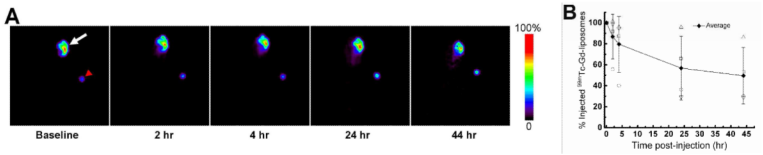

Figure 6.

Planar gamma camera images of SCCHN xenografted nude rats intratumorally infused with ^{99m}Tc-Gd-liposomes (white arrow: tumor; red arrow head: reference standard outside the animal body) (**A**) and the intratumoral retention of injected ^{99m}Tc radioactivity with time (**B**).

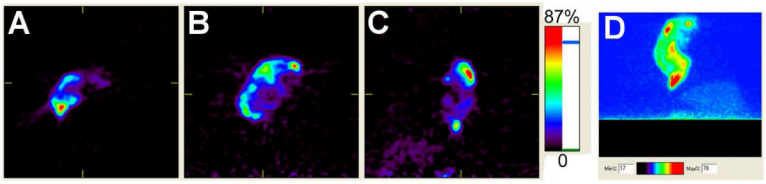

Figure 7.
Micro-PET images depicting the locoregional retention of the ^{64}Cu-Gd-liposomes 24 hr after intratumoral infusion (**A**, **B**, **C**, and **D** show the axial, coronal, sagittal, and projection images, respectively).